Optics Communications 282 (2009) 18–21

Contents lists available at ScienceDirect

Optics Communications

journal homepage: www.elsevier.com/locate/optcom

Optimization of the operational bandwidth in air-core photonic bandgap fibers for IR transmission

Jonathan Hu *, Curtis R. Menyuk

Department of Computer Science and Electrical Engineering, University of Maryland Baltimore County, 5200 Westland Boulevard 205A, Baltimore, MD 21250, USA

ARTICLE INFO

Article history:
Received 25 July 2008
Received in revised form 9 September 2008
Accepted 9 September 2008

Keywords:
Fiber design and fabrication
Infrared
Fiber properties

ABSTRACT

We determine the optimal inner glass ring thickness in infrared air-core photonic bandgap fibers (PBGFs) with 19-cell and 7-cell cores. For PBGFs with a 19-cell core, we find that an inner ring thickness of 0.04 Λ, where Λ is pitch, yields the widest operational bandwidth, which is nearly 6%. The operational bandwidth increases as the refractive index decreases from 2.8 to 2.0. For PBGFs with a 7-cell core, one needs to draw fiber with a ring thickness of less than 0.03 Λ to achieve a comparable operational bandwidth.

1. Introduction

Air-core photonic bandgap fibers (PBGFs), in contrast to some other types of holey fiber, guide light through the photonic bandgap effect, instead of using total internal reflection [1]. These air-core PBGFs have the potential to provide very low-loss transmission, along with delivery of high-powers and low-nonlinearity.

Surface modes, which are located between the core and cladding, have been shown to have a significant impact on the loss of the fundamental mode [2,3]. Amezcua-Correa et al. [4–6] demonstrated that by carefully selecting the thickness of the inner glass ring around the core, it is possible to push the surface modes away from the center of the bandgap in silica PBGFs. Laser-power delivery in infrared (IR) region through optical fibers has important military and medical applications [7,8]. Pearce et al. [9] showed that a PBGF with a 19-cell core and a glass refractive index of 2.4 has an operational bandwidth of 5% of the center frequency with an inner glass ring thickness of 0.05 Λ, where the pitch, Λ, is defined as the distance between the centers of the nearby holes. However, this result does not indicate what parameter choice optimizes the bandwidth. In this paper, we study the operational bandwidth as a function of inner glass ring thickness for PBGFs with different refractive indices for the glasses used for IR transmission. We analyze fibers with both a 19-cell and a 7-cell core. These geometries were previous studied [4,9]. The optimum inner glass ring thickness that yields the widest operational bandwidth is 0.04 Λ. We consider non-silica glasses that have a refractive index between 2.0 and 2.8 [10]. The operational bandwidth increases when the refractive index decreases from 2.8 to 2.0, which is slightly larger than the range of possible values of chalcogenide glass used for IR transmission [7].

2. Fiber geometry

We calculate the fiber modes and their propagation constants using Comsol Multiphysics, a commercial full-vector mode solver based on the finite-element method. Anisotropic perfectly-matched layers (PMLs) [11] are positioned outside the outermost ring of holes in order to reduce the simulation window for a PBGF with five air-hole rings. To validate our simulations, we compared our results to Fig. 3 of Ref. [4], and we obtained agreement. Fig. 1 shows the fiber core geometries for two air-core PBGFs. The core is created by introducing a larger air hole at the center of the fiber. Only a quarter of the geometry is used in modeling PBGFs because of the symmetry of the fundamental core mode. Modes of other symmetry classes do exist within the bandgap, but it is expected that they will have little impact on the usable bandwidth. Fig. 1a and b correspond to a 19-cell and 7-cell core, meaning that 19 and 7 air holes have been removed, respectively, to form the core before the drawing process. In this study we use $D/\Lambda = 0.8$ for both 19-cell and 7-cell cores, which has been shown to yield a wide bandgap for high-index glass [12]. In Fig. 1a, the corner of the inner glass ring is rounded with radius d_p, where $d_p/\Lambda = 0.5$. In Fig. 1b, we use $d_p/\Lambda = 0.2$. The corner of the core region is rounded with radius d_c, where $d_c/\Lambda = 0.94$.

3. Result and analysis

When there is no coupling loss due to surface modes, the overall attenuation is dominated by scattering loss due to surface

* Corresponding author. Tel.: +1 410 455 6507; fax: +1 410 455 6500.
E-mail address: hu1@umbc.edu (J. Hu).

0030-4018/$ - see front matter © 2008 Elsevier B.V. All rights reserved.
doi:10.1016/j.optcom.2008.09.055

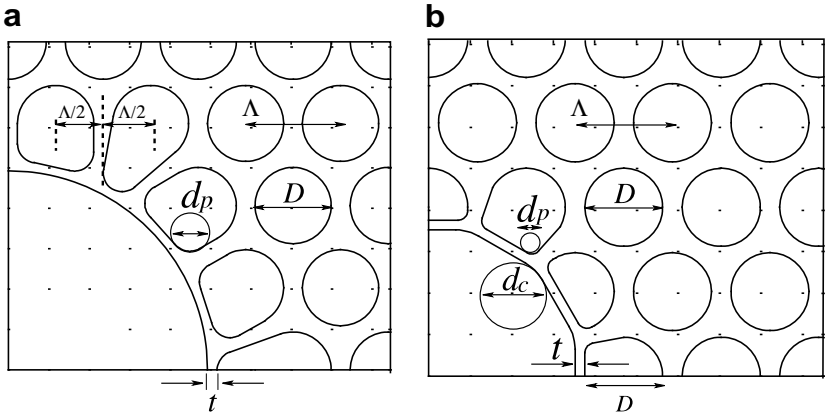

Fig. 1. Fiber geometries for PBGFs with (a) a 19-cell core and (b) a 7-cell core.

roughness. This loss factor F can be estimated from the field intensity at the air–glass interfaces as [13]

$$F = \left(\frac{\epsilon_0}{\mu_0}\right)^{1/2} \frac{\oint_{\text{hole perimeters}} dl|\mathbf{E}|^2}{\left|\int_{\text{cross-section}} dA(\mathbf{E}\times\mathbf{H}^*)\cdot\hat{\mathbf{z}}\right|}, \quad (1)$$

where ϵ_0 and μ_0 are the vacuum permittivity and permeability, respectively, while **E** and **H** denote the electric and magnetic field. In the numerator, the **E**-field is evaluated along the path just inside each hole interface. Fig. 2 shows the power in the core as a percentage of the total power and the normalized loss factor $F\cdot\Lambda$. The refractive index of the glass is set equal to 2.4. As the normalized ring thickness t/Λ increases, the number of surface modes also increases. When t/Λ is larger than 0.08, the increase in the number of surface modes leads to a decrease in the operational bandwidth. In Fig. 2a,[1] we use red to indicate the parameter range where the fundamental core mode has more than 90% of power located in the core. Yellow indicates avoided crossings due to the surface modes [3]. Blue indicates the parameter range where the fundamental mode is no longer confined in the core. Note that Fig. 2a and b are highly correlated. In Fig. 3a, we show the mode effective index as a function of normalized frequency at a normalized ring thickness of 0.05. The blue solid and dashed curves represent the fundamental air-guided mode and surface modes, respectively. The black dashed lines represent the edge of the bandgap, calculated by the full-vectorial plane-wave method [14]. This fiber has an avoided crossing between the fundamental mode and a surface mode within the bandgap at a normalized frequency of 0.9. Away from the avoided crossing point, most of the optical power of the fundamental mode is localized in the core region, as shown in mode (I). The surface mode (III) has most of its power confined in the glass region between the core and the cladding. At a frequency near the avoided crossing, the mode shown in (II) cannot be unambiguously identified as either a core mode or a surface mode, since the power is distributed in both the core and surface regions. In Fig. 3b, we show both power in the core and the normalized loss factor $F\cdot\Lambda$. These two quantities are inversely related. We obtain the optimal normalized ring thickness that yields the widest possible operational bandwidth where $F\cdot\Lambda$ is maintained below 1.6. The optimal bandwidth is insensitive to the threshold value of 1.6 for $F\cdot\Lambda$, as is apparent in Fig. 3. The power in the core is more than 90% of the total power in this case. We define the relative operational bandwidth as the ratio of the widest operational bandwidth to the center frequency. Fig. 4 shows the relative operational bandwidth as a function of normalized ring thickness with glass refractive indices of 2.2, 2.3, 2.4, and 2.5. Note that the optimal normalized ring thickness is 0.04, which yields a relative operational bandwidth of nearly 6% for a refractive index of 2.4. Fig. 5 shows that the relative operational bandwidth as a function of refractive index at a ring thickness of 0.04. The relative operational bandwidth increases as the refractive index decreases from 2.8 to 2.0.

In Fig. 6, we present the power in the core and the normalized loss factor $F\cdot\Lambda$ for a PBGF with a 7-cell core and a glass refractive

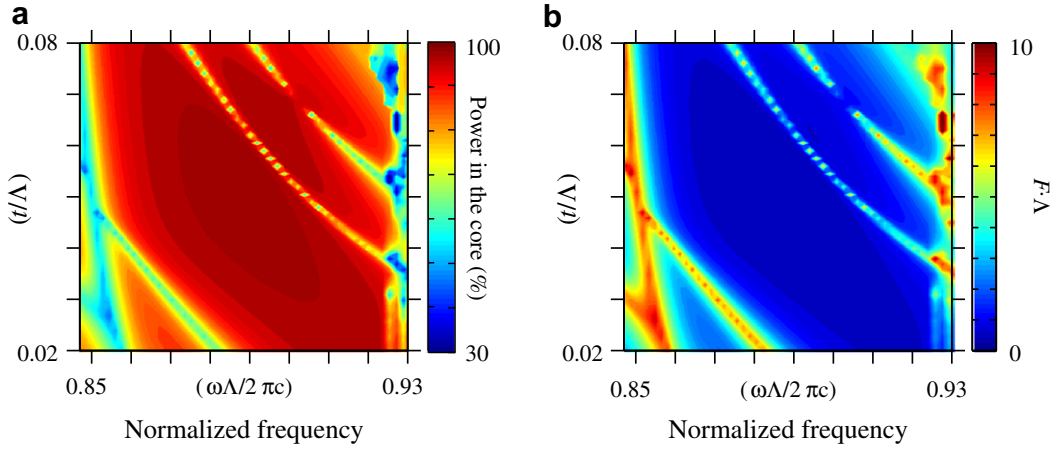

Fig. 2. Contour plots of (a) power in the core and (b) $F\cdot\Lambda$ for a PBGF with a 19-cell core. The refractive index of the glass equals 2.4.

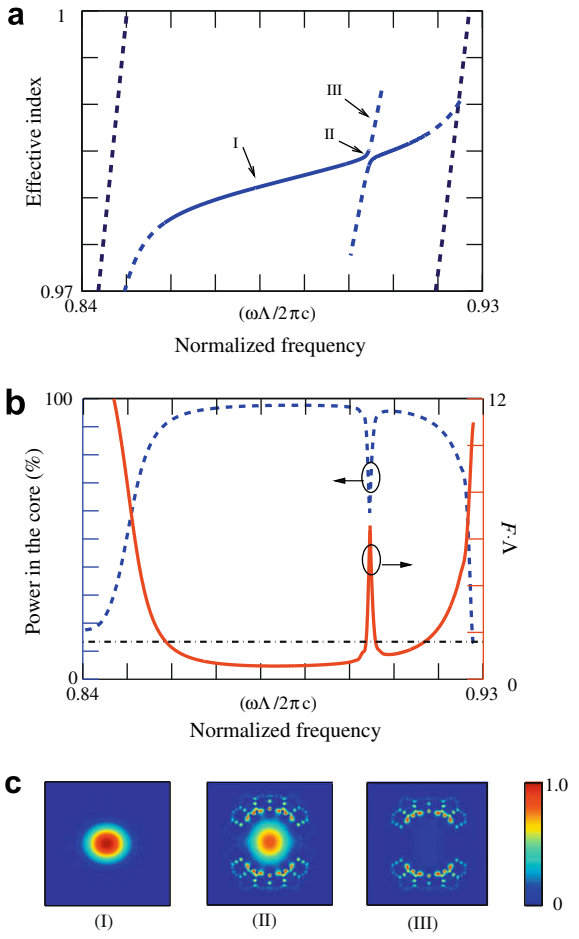

Fig. 3. (a) The mode effective index as a function of normalized frequency at a normalized ring thickness of 0.05. The blue solid and dashed curves represent the fundamental air-guided mode and surface modes, respectively. The black dashed lines represent the edge of the bandgap. (b) The comparison between power in the core and normalized factor $F \cdot \Lambda$ for a PBGF with a 19-cell core. Black dash-dotted line indicates $F \cdot \Lambda = 1.6$. (c) The relative mode intensity profiles correspond to points I, II, and III in (a).

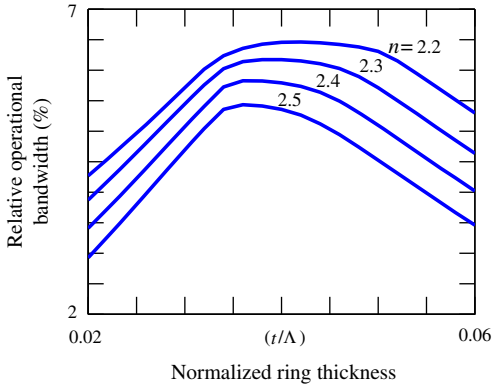

Fig. 4. Relative operational bandwidth as a function of normalized ring thickness.

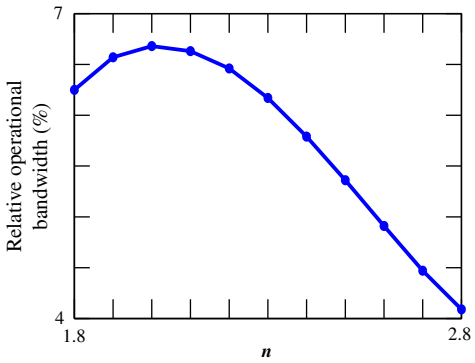

Fig. 5. The relative operational bandwidth for different glass refractive indices with a normalized ring thickness of 0.04.

index of 2.4. In this case, when the normalized ring thickness is less than 0.05, the relative operational bandwidth increases as the normalized ring thickness decreases. The relative operational bandwidth is higher than 6% when the normalized ring thickness is less than 0.03. Such a small ring thickness may be difficult to draw in practice.

4. Conclusion

For PBGFs with a 19-cell core, a normalized ring thickness of 0.04 yields the widest operational bandwidth, which is nearly 6%. The operational bandwidth increases as the refractive index decreases from 2.8 to 2.0. For PBGFs with a 7-cell core, one must

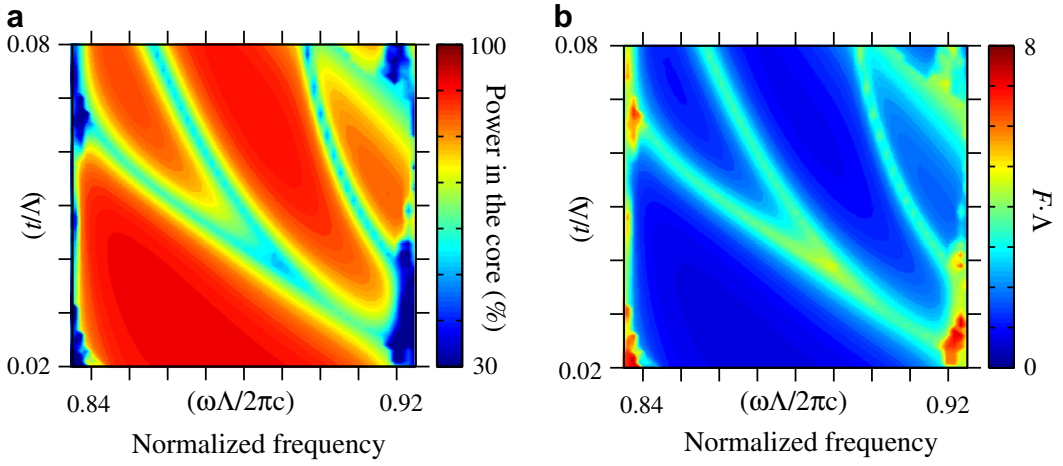

Fig. 6. Contour plots of (a) power in the core and (b) $F \cdot \Lambda$ for a PBGF with a 7-cell core.

draw fiber with a ring thickness of less than 0.03 Λ to achieve a comparable operational bandwidth.

Acknowledgements

The authors would like to thank Rodrigo Amezcua-Correa for helping us to compare his group's simulation results to ours. This work has been partially supported by the Naval Research Laboratory.

References

[1] J. Broeng, S.E. Barkou, T. Sondergaard, A. Bjarklev, Opt. Lett. 25 (2000) 96.
[2] K. Saitoh, N. Mortensen, M. Koshiba, Opt. Express 12 (2004) 394.
[3] J. West, C. Smith, N. Borrelli, D. Allan, K. Koch, Opt. Express 12 (2004) 1485.
[4] R. Amezcua-Correa, N.G. Broderick, M.N. Petrovich, F. Poletti, D.J. Richardson, Opt. Express 14 (2006) 7974.
[5] R. Amezcua-Correa, N.G. Broderick, M.N. Petrovich, F. Poletti, D.J. Richardson, Opt. Express 15 (2007) 17577.
[6] R. Amezcua-Correa, F. Gèrôme, S.G. Leon-Saval, N.G.R. Broderick, T.A. Birks, J.C. Knight, Opt. Express 16 (2008) 1142.
[7] J.S. Sanghera, I.D. Aggarwal, L.E. Busse, P.C. Pureza, V.Q. Nguyen, F.H. Kung, L.B. Shaw, F. Chenard, Laser Focus World 41 (2005) 83.
[8] C. Anastassiou, G. Dellemann, O. Weisberg, U. Kolodny, Photon. Spectra 38 (2004) 108.
[9] G. Pearce, J. Pottage, D. Bird, P. Roberts, J. Knight, P.J. Russell St, Opt. Express 13 (2005) 6937.
[10] X. Feng, A.K. Mairaj, D.W. Hewak, T.M. Monro, J. Lightwave Technol. 23 (2005) 2046.
[11] K. Saitoh, M. Koshiba, Opt. Express 11 (2003) 3100.
[12] J. Hu, C.R. Menyuk, Opt. Express 15 (2007) 339.
[13] P. Roberts, F. Couny, H. Sabert, B. Mangan, D. Williams, L. Farr, M. Mason, A. Tomlinson, T. Birks, J. Knight, P.J. Russell St, Opt. Express 13 (2005) 236.
[14] S. Johnson, J. Joannopoulos, Opt. Express 8 (2001) 173.